23rd International Symposium on Mathematical Theory of Networks and Systems
Hong Kong University of Science and Technology, Hong Kong, July 16-20, 2018

Characterization of isothermal CO_2 sorption columns by simultaneous spatiotemporal modeling of transient capacity and heat flow

Manda Yang[1], Linxi Wang[1], Robert M. Rioux[1,2,⋆] and Antonios Armaou[1,3,⋆]

***Abstract*— We relax several assumptions in the model from our previous work that was published in 2016 to model isothermal CO_2 adsorption columns based on breakthrough curves and calorimetry measurements. The unknown parameters in the models are determined by minimizing the integral in time of the squared difference between the model prediction and experimental measurement. In a previous effort, only the CO_2 adsorption behavior was used to develop the model. In this work, we include calorimetry data to improve the model. Based on the simulation result and theoretical prediction, we conclude that physical adsorption and/or elementary reactions may need to be considered in the model.**

I. Introduction

In recent years, extensive research effort has been dedicated to CO_2 capture technology due to CO_2's contribution to global climate change [13], [15], [29]. Technologies to mitigate CO_2 include pre-combustion carbon capture, post-combustion carbon capture and oxy-combustion [19], [20], [11]. Compared with other technologies, post-combustion carbon capture has the advantages of easier implementation in existing plants and maintenance operations don't require main plant operation cycle to shut down [3]. Post-combustion capture materials include membranes [28], CO_2 capture sorbents [5], [14], metal organic frameworks[30], enzyme-based system [1], aqueous ammonia [10], [16] and Higee technology [31]. While aqueous ammonia is a mature technology, CO_2 capture sorbents have less causticity and consume less energy during CO_2 desorption [31].

To understand and predict the dynamics of CO_2 sorption in a fixed bed column, many models have been proposed in the literature [17], [7], [12], [27], [3], [21], [9], [26], [6]. In Heydari-Gorji's work [12], an adsorption model based on Avrami's equation was proposed. In Monazam's work [23], different adsorption models were compared to determine the equilibrium relationships between sorbent and sorbate; the adsorption rate was considered to be a function of CO_2 concentration, fraction of sites which are occupied by adsorbed gas and temperature. However, axial dispersion in the bed wasn't considered. Knox's work [18] considered axial dispersion in the bed, but an unphysical assumption of linear driving force was made. Bollini and coworkers considered both heat and mass transfer in their model [4], but they were unable to capture the temperature profile in their model. In previous work by our group [2], we proposed a model to circumvent the unphysical assumptions of linear driving force and uniform adsorption rates; unknown parameters were determined using the breakthrough curves; however the heat released as measured by microcalorimetry due to adsorption couldn't be accurately captured by the model.

The current work attempts to improve the accuracy of our previous model. It relaxes some assumptions that were made in that model, and then considers different reaction mechanisms to describe the experimental observations. Physical quantities are estimated (including CO_2 adsorption capacity, relevant rate constants and heat of reaction) by minimizing the deviation of the model prediction from the experiment measurements in time. In our previous model, we only looked at the concentration of CO_2 when it's being adsorbed by the reactor. To provide a richer behavior for estimation, we also utilized the concentration of CO_2 when it's being desorbed and the associated calorimetry profiles at various temperatures.

II. Experimental apparatus

The adsorption behavior of CO_2 was studied in a home-built breakthrough reactor (BTR) with PEI-impregnated SiO_2 in it. A pulse of CO_2 was introduced to the packed bed through a 10-way valve which switches between the purge gas and adsorptive gas (10% CO_2/1% Ar/He). Ar served as a tracer gas in order to accurately determine the total CO_2 capacity of the packed bed and correct for valve dynamics. The effluent gas was monitored with a mass spectrometer. A differential scanning calorimeter was used to measure the transient heat flow necessary to maintain the packed bed at isoperibol conditions. BTR curves were measured at 25°C, 40°C, 50°C, 60°C, 70°C and 80°C.

III. Derivation of BTR spatiotemporal model

In order to derive a physically relevant model we avoided implementing unphysical assumptions made in other reports [4], [12], [18]. However, to reduce model complexity we did make the following assumptions

1) The process is isothermal.

M.Y. and A.A. acknowledge the financial support from the National Science foundation, CMMI award #13-00322. A.A. acknowledges the financial support from Zhejiang Provincial Thousand Foreign Talents Program, and Chinese National Fund Award, High-end Foreign Experts Program. L. W. and R. M. R. acknowledge the US National Science Foundation (NSF grant # CBET-1551119) for financial support of this work. Additional support of this work was provided to R. M. R. by the Institutes for Energy and the Environment at the Pennsylvania State University. We acknowledge McMahan Gray and James Hoffman from the National Energy Technology Laboratory for the PEI423 material.

[1]Department of Chemical Engineering, The Pennsylvania State University, University Park, PA 16802, USA; [2]Department of Chemistry, The Pennsylvania State University, University Park, PA 16802; [3]Department of Mechanical Engineering, Wenzhou University, Zhejiang, China; ⋆corresponding author, Email address: rioux@engr.psu.edu, armaou@engr.psu.edu

2) CO_2 concentration gradient in the axial direction is considered; radial gradients can be neglected.
3) Helium and Argon do not sorb.
4) The transport behavior (dispersion, convection) of Helium and Argon are identical.
5) The thermodynamic behavior of all gaseous species can be described by the ideal gas equation of state.

To extend our previous results [2] and improve the accuracy of the proposed model, we relaxed the following assumptions

(i) The total concentration of accessible sites on the sorbent column remains constant.
(ii) The superficial velocity is uniform in space.

To justify relaxing Assumption (i) we considered that although the *total* concentration of the active sites should be the same at different temperatures, the higher kinetic barrier for the diffusion of CO_2 at lower temperatures reduces the number of accessible sites. [22]

Based on Assumption 3 and 5, the concentration of Ar will increase when CO_2 is sorbed, therefore the superficial velocity will decrease (Assumption ii).

A. Transport equation

Based on the mole balance, we can obtain: [2]

$$\frac{\partial C_{\mathrm{CO_2}}}{\partial t} = -\frac{\partial F_{\mathrm{CO_2}z}}{\partial z} - \frac{1-\epsilon}{\epsilon}\rho_b r_{ads} \tag{1}$$

where z is the distance in axial direction of the bed, t denotes time, $C_{\mathrm{CO_2}}$ refers to the concentration of CO_2 in the gas phase. $F_{\mathrm{CO_2}z}$ is the molar flow rate @ z. $\rho_b[kg_{cat}/m^3]$ denotes the density of the bed and r_{ads} is the adsorption rate of CO_2. ϵ refers to the void fraction. By applying Fick's first law,

$$F_{\mathrm{CO_2}z} = -D_L\frac{\partial C_{\mathrm{CO_2}}}{\partial z} + u_i C_{\mathrm{CO_2}} \tag{2}$$

where $u_i = \frac{u_s}{\epsilon}$ denotes the interstitial velocity and u_s is the superficial velocity. The axial dispersion coefficient D_L is determined by

$$D_L = \gamma_1 D_m + 2\gamma_2 R_p u_i \tag{3}$$

where $\gamma_1 = 0.45 + 0.55\epsilon$ and $g2 = 0.5$ [24]. To consider the dependence of diffusion coefficient D_m on temperature, Chapman-Enskog theory is applied. By substituting Eq.2 in Eq. 1, we obtain

$$\begin{aligned}\frac{\partial C_{\mathrm{CO_2}}}{\partial t} = D_L\frac{\partial^2 C_{\mathrm{CO_2}}}{\partial z^2} - \frac{u_s}{\epsilon}\frac{\partial C_{\mathrm{CO_2}}}{\partial z} \\ - \frac{C_{\mathrm{CO_2}}}{\epsilon}\frac{\partial u_s}{\partial z} - \frac{1-\epsilon}{\epsilon}\rho_b r_{\mathrm{ads}}\end{aligned} \tag{4}$$

The superficial velocity varies in space because of the adsorption and desorption of CO_2. We assume the pressure drop is negligible; therefore:

$$C_{\mathrm{CO_2}} + C_{\mathrm{He}} + C_{\mathrm{Ar}} = \mathrm{const.} \tag{5}$$

We assume the concentration change over time of He and Ar is negligible; therefore the molar flow rates of He and Ar are uniform. The superficial velocity over space becomes

$$u_s|_0(C_{\mathrm{He}}|_0 + C_{\mathrm{Ar}}|_0) = u_s(C_{\mathrm{He}}|_0 + C_{\mathrm{Ar}}|_0 + C_{\mathrm{CO_2}}|_0 - C_{\mathrm{CO_2}}) \tag{6}$$

B. reaction mechanism

In this work, we modified the one reaction mechanism used in our previous work, called dual-site chemisorption scheme. It is the common carbamate mechanism with no distinction as to the nature of amine sites. Since the elementary reactions are lumped into one reaction, the number of parameters in the model is reduced.

$$\mathrm{CO_2(g)} + 2\,\mathrm{S} \underset{k_{-1}}{\overset{k_1}{\rightleftharpoons}} \mathrm{S(CO_2)S} \quad \Delta\mathrm{H} \tag{7}$$

where S refers to site and S(CO_2)S refers to one molecular of CO_2 is adsorbed to two sites.

The overall adsorption rate is

$$r_{ads} = k_1 P_{\mathrm{CO_2}} C_{\mathrm{S}}^2 - k_{-1} C_{\mathrm{S(CO_2)S}} \tag{8}$$

Previously [2], the equilibrium adsorption constant was used to reduce the number of unknown parameters in the model. Presently, we no longer use such constants because the reactions are not at equilibrium after breakthrough. Another reason is the calculated total amount of adsorbed CO_2 may not be accurate because of the baseline change and the long tail in the breakthrough curves.

C. parameter estimation

Prior to each adsorption experiment, we purged pure helium through the reactor. When the adsorption experiment begins at $t = 0$, adsorptive gas that contains CO_2, Ar and He enters the reactor; at $t = t_1$, the sample is saturated and the concentration of CO_2 in the outlet reaches maximum; at $t = t_2$ the gas will be switched back to pure He. We call $[0\ \ t_1]$ "upswing" ; $[t_1\ \ t_2]$ "plateau period" ; $[t_2\ \ t_3]$ is called "downswing" . Since the length of plateau period (around 9000s) is much longer than upswing (around 300s) and downswing (around 1000s), we only consider the deviation of the estimated breakthrough curve and heat profile from the experiment result during the upswing and the downswing. The integral of the deviation over time is balanced by the length of each period so that the data in the upswing and the downswing is equally weighted when solving the problem. The unknown parameters are determined by minimizing the deviation (Eq. 9).

The unknown parameters include rate constants (k_1, k_{-1}), heat of sorption (ΔH), total number of sites (C_t) and dt, which is used to align the heat flow data stream and the breakthrough curve data stream. We denote the set of unknown parameters by U_i, where i indicates a different

experimental temperature

$$U_i^* = \underset{U_i}{arg\,min}\Bigg(\alpha\Big(\frac{1}{t_1(C^{exp}_{\mathrm{CO}_2,max,up})^2}\int_0^{t_1}(C_{\mathrm{CO}_2}(L,t) - C^{exp}_{\mathrm{CO}_2}(L,t))^2\mathrm{d}t + \frac{1}{(t_3-t_2)(C^{exp}_{\mathrm{CO}_2,max,down})^2}\int_{t_2}^{t_3}(C_{\mathrm{CO}_2}(L,t) - C^{exp}_{\mathrm{CO}_2}(L,t))^2\mathrm{d}t\Big) + \Big(\frac{1}{t_1(Q^{exp}_{T_i,max,up})^2}\int_0^{t_1}(Q_{T_i}(t) - Q^{exp}_{T_i}(L,t))^2\mathrm{d}t + \frac{1}{(t_3-t_2)(Q^{exp}_{T_i,max,down})^2}\int_{t_2}^{t_3}(Q_{T_i}(t) - Q^{exp}_{T_i}(t))^2\mathrm{d}t\Big)\Bigg) \tag{9}$$

where $C_{\mathrm{CO}_2 max}$ and $Q_{T_i max}$ denote the maximum of breakthrough curves and heat profile at $T = T_i$. The superscript exp refers to the experiment result and superscript $*$ denotes optimal values. When $\alpha = 1$, the deviation of the breakthrough curve and heat flow profile are penalized equally in the optimization problem. When the concentration of CO_2 in the outlet increases to the maximum, the error of all the models becomes negligible; yet the model prediction of heat flow does not match the experiment result. Because of this, the values of the last 2 terms in Eq. 9 are larger than those of the first 2 terms if α is 1, which will result in the better fit of heat flow profile than the breakthrough curves because the deviation of heat flow profile are penalized more compared with the deviation of breakthrough curves. To balance the two different data streams we choose $\alpha = 10$.

IV. Result and discussion

The simulation prediction and experiment result of the breakthrough curves and heat profile is given in Fig. 1. It can be seen the model capture the experiment behavior very well. However, the determined rate constant of the forward reaction decreases as temperature increases, which doesn't obey the Arrhenius equation. One of the explanations is the activation energy of reverse reaction is larger than that of the forward reaction [25] since the reaction in our model is a lump of many reactions. Another possible reason is CO_2 has to be physically adsorbed first before it reacts with amine [8]. Physically adsorption rate decreases as temperature increases, which results in the apparent negative activation energy. To address this issue, physical adsorption and/or elementary reactions may need to be considered in the model.

V. Conclusions

In this work, we relaxed an assumption in the previous work improve the accuracy of the model for CO_2 sorption, and determined the unknown parameters by minimizing the deviation of the model prediction from the experiment result. The prediction fits the experiment result, but suffers from the negative activation problem. Physical adsorption and/or elementary reactions may need to be considered to address this issue.

References

[1] Aaron M. Appel, John E. Bercaw, Andrew B. Bocarsly, Holger Dobbek, Daniel L. Dubois, Michel Dupuis, James G. Ferry, Etsuko Fujita, Russ Hille, Paul J.A. Kenis, Cheryl A. Kerfeld, Robert H. Morris, Charles H.F. Peden, Archie R. Portis, Stephen W. Ragsdale, Thomas B. Rauchfuss, Joost N.H. Reek, Lance C. Seefeldt, Rudolf K. Thauer, and Grover L. Waldrop. Frontiers, opportunities, and challenges in biochemical and chemical catalysis of CO_2 fixation. *Chemical Reviews*, 113(8):6621–6658, 2013.

[2] Davood Babaei Pourkargar, Seyed Mehdi Kamali Shahri, Robert M. Rioux, and Antonios Armaou. Spatiotemporal Modeling and Parametric Estimation of Isothermal CO_2 Adsorption Columns. *Industrial and Engineering Chemistry Research*, 55(22):6443–6453, jun 2016.

[3] R. Ben-Mansour, M. A. Habib, O. E. Bamidele, M. Basha, N. A.A. Qasem, A. Peedikakkal, T. Laoui, and M. Ali. Carbon capture by physical adsorption: Materials, experimental investigations and numerical modeling and simulations - A review. *Applied Energy*, 161:225–255, 2016.

[4] P Bollini, N A Brunelli, S A Didas, and C W Jones. Dynamics of CO_2 Adsorption on Amine Adsorbents. 1. Impact of Heat Effects. *Industrial & Engineering Chemistry Research*, 51(46):15145–15152, 2012.

[5] Zhenhe Chen, Shubo Deng, Haoran Wei, Bin Wang, Jun Huang, and Gang Yu. Polyethylenimine-impregnated resin for high CO2 adsorption: An efficient adsorbent for CO_2 capture from simulated flue gas and ambient air. *ACS Applied Materials and Interfaces*, 5(15):6937–6945, 2013.

[6] Tirzhá L P Dantas, Francisco Murilo T Luna, Ivanildo J. Silva, Antonio Eurico B Torres, Diana C S de Azevedo, Alírio E. Rodrigues, and Regina F P M Moreira. Carbon dioxide-nitrogen separation through pressure swing adsorption. *Chemical Engineering Journal*, 172(2-3):698–704, 2011.

[7] Tirzhá L.P. Dantas, Francisco Murilo T. Luna, Ivanildo J. Silva, Diana C.S. de Azevedo, Carlos A. Grande, Alírio E. Rodrigues, and Regina F.P.M. Moreira. Carbon dioxide-nitrogen separation through adsorption on activated carbon in a fixed bed. *Chemical Engineering Journal*, 169(1-3):11–19, 2011.

[8] A D Ebner, M L Gray, N G Chisholm, Q T Black, D D Mumford, M A Nicholson, and J A Ritter. Suitability of a Solid Amine Sorbent for CO_2 Capture by Pressure Swing Adsorption. *Industrial & Engineering Chemistry Research*, 50(9):5634–5641, 2011.

[9] Yanfang Fan, Jayashree Kalyanaraman, Ying Labreche, Fateme Rezaei, Ryan P. Lively, Matthew J. Realff, William J. Koros, Christopher W. Jones, and Yoshiaki Kawajiri. CO_2 sorption performance of composite polymer/aminosilica hollow fiber sorbents: An experimental and modeling study. *Industrial and Engineering Chemistry Research*, 54(6):1783–1795, 2015.

[10] José D. Figueroa, Timothy Fout, Sean Plasynski, Howard McIlvried, and Rameshwar D. Srivastava. Advances in CO_2 capture technology-The U.S. Department of Energy's Carbon Sequestration Program. *International Journal of Greenhouse Gas Control*, 2(1):9–20, 2008.

[11] Susana Garcia, Eva Sanchez Fernandez, Alisdair J. Stewart, and M. Mercedes Maroto-Valer. Process Integration of Post-combustion CO_2 Capture with Li_4SiO_4/Li_2CO_3 Looping in a NGCC Plant. *Energy Procedia*, 114(November 2016):2611–2617, 2017.

[12] Aliakbar Heydari-Gorji and Abdelhamid Sayari. CO_2 capture on polyethylenimine-impregnated hydrophobic mesoporous silica: Experimental and kinetic modeling. *Chemical Engineering Journal*, 173(1):72–79, 2011.

[13] Bjart Holtsmark. Quantifying the global warming potential of CO_2 emissions from wood fuels. *GCB Bioenergy*, 7(2):195–206, 2015.

[14] Yu Jing, Li Wei, Yundong Wang, and Yanmei Yu. Synthesis, characterization and CO_2 capture of mesoporous SBA-15 adsorbents functionalized with melamine-based and acrylate-based amine dendrimers. *Microporous and Mesoporous Materials*, 183:124–133, 2014.

[15] F. Joos, R. Roth, J. S. Fuglestvedt, G. P. Peters, I. G. Enting, W. Von Bloh, V. Brovkin, E. J. Burke, M. Eby, N. R. Edwards, T. Friedrich, T. L. Frölicher, P. R. Halloran, P. B. Holden, C. Jones, T. Kleinen, F. T. Mackenzie, K. Matsumoto, M. Meinshausen, G. K. Plattner, A. Reisinger, J. Segschneider, G. Shaffer, M. Steinacher, K. Strassmann, K. Tanaka, A. Timmermann, and A. J. Weaver. Carbon dioxide and climate impulse response functions for the computation of greenhouse gas metrics: A multi-model analysis. *Atmospheric Chemistry and Physics*, 13(5):2793–2825, 2013.

[16] Johannes Kainz, Patrick David, Leonidas Werz, Carsten Troll, and Bernhard Rieger. Temperature and CO_2 responsive polyethylenimine for highly efficient carbon dioxide release. *RSC Advances*, 5:9556–9560, 2015.

[17] J Kalyanaraman, Y Fan, Y Labreche, R P Lively, Y Kawajiri, and M J Realff. Bayesian estimation of parametric uncertainties, quantification and reduction using optimal design of experiments for CO_2 adsorption on amine sorbents. *Computers & Chemical Engineering*, 81:376–388, 2015.

[18] James C Knox, Armin D Ebner, M. Douglas Levan, Robert F Coker, and James A Ritter. Limitations of Breakthrough Curve Analysis in Fixed-Bed Adsorption. *Industrial and Engineering Chemistry Research*, 55(16):4734–4748, 2016.

[19] Shreenath Krishnamurthy, Vemula Rama Rao, Sathishkumar Guntuka, Paul Sharratt, Reza Haghpanah, Arvind Rajendran, Mohammad Amanullah, Iftekhar A. Karimi, and Shamsuzzaman Farooq. CO2 Capture from Dry Flue Gas by Vacuum Swing Adsorption: A Pilot Plant Study. *AIChE J*, 60(5):1830–1842, 2014.

[20] Dennis Y.C. Leung, Giorgio Caramanna, and M. Mercedes Maroto-Valer. An overview of current status of carbon dioxide capture and storage technologies. *Renewable and Sustainable Energy Reviews*, 39:426–443, 2014.

[21] B. Liu, X. Luo, Z. Liang, W. Olson, H. Liu, R. Idem, and P. Tontiwachwuthikul. The development of kinetics model for CO_2 absorption into tertiary amines containing carbonic anhydrase. *AIChE Journal*, 63(11):4933–4943, 2017.

[22] Xiaoliang Ma, Xiaoxing Wang, and Chunshan Song. Molecular Basket Sorbents for Separation of CO_2 and H_2S from Various Gas Streams. *J. Am. Chem. Soc.*, 131(13):5777–5783, 2009.

[23] Esmail R Monazam, Lawrence J Shadle, David C Miller, Henry W Pennline, Daniel J Fauth, James S Hoffman, and Mcmahan L Gray. Equilibrium and Kinetics Analysis of Carbon Dioxide Capture using Immobilized Amine on a Mesoporous Silica. *AIChE Journal*, 59(3):923–925, 2013.

[24] Douglas M Ruthven. *Principles of adsorption and adsorption processes*. John Wiley & Sons, 1984.

[25] Mehdi Sedighi, Kamyar Keyvanloo, and Jafar Towfighi. Kinetic study of steam catalytic cracking of naphtha on a Fe/ZSM-5 catalyst. *Fuel*, 109:432–438, 2013.

[26] R Serna-Guerrero and A Sayari. Modeling adsorption of CO_2 on amine-functionalized mesoporous silica. 2: Kinetics and breakthrough curves. *Chemical Engineering Journal*, 161(1-2):182–190, 2010.

[27] Rodrigo Serna-Guerrero, Youssef Belmabkhout, and Abdelhamid Sayari. Modeling CO_2 adsorption on amine-functionalized mesoporous silica: 1. A semi-empirical equilibrium model. *Chemical Engineering Journal*, 161(1-2):173–181, 2010.

[28] Jie Shen, Gongping Liu, Kang Huang, Wanqin Jin, Kueir Rarn Lee, and Nanping Xu. Membranes with fast and selective gas-transport channels of laminar graphene oxide for efficient CO_2 capture. *Angewandte Chemie - International Edition*, 54(2):578–582, 2015.

[29] Keith P. Shine. The global warming potential-the need for an interdisciplinary retrial. *Climatic Change*, 96(4):467–472, 2009.

[30] Junya Wang, Liang Huang, Ruoyan Yang, Zhang Zhang, Jingwen Wu, Yanshan Gao, Qiang Wang, Dermot O'Hare, and Ziyi Zhong. Recent advances in solid sorbents for CO_2 capture and new development trends. *Energy Environ. Sci.*, 7(11):3478–3518, 2014.

[31] Cheng Hsiu Yu, Chih Hung Huang, and Chung Sung Tan. A Review of CO_2 Capture by Absorption and Adsorption. *Aerosol and Air Quality Research*, 12(5):745–769, 2012.

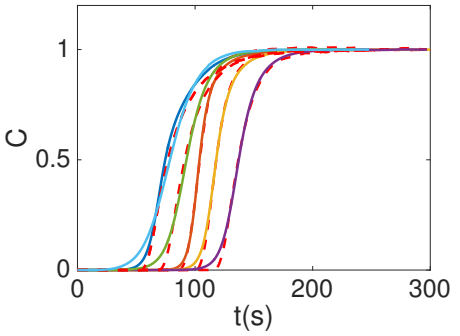

(a) breakthrough curves of the upswing.

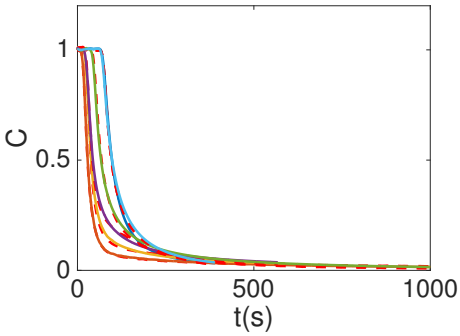

(b) breakthrough curves of the downswing.

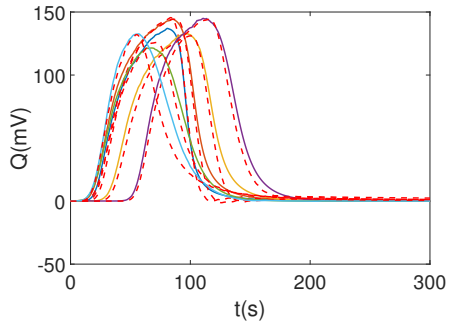

(c) heat flow of the upswing.

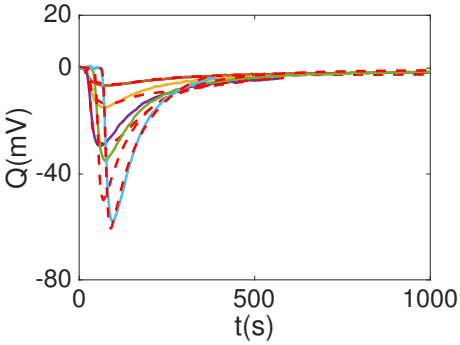

(d) heat flow of the downswing.

Fig. 1: Temporal profiles of experimentally observed normalized concentration of CO_2 and respective heat flow during upswing and downswing for different temperatures presented with dashed red lines, and the respective simulation predictions presented with solid lines.